

Dalton Transactions

Accepted Manuscript



This is an *Accepted Manuscript*, which has been through the Royal Society of Chemistry peer review process and has been accepted for publication.

Accepted Manuscripts are published online shortly after acceptance, before technical editing, formatting and proof reading. Using this free service, authors can make their results available to the community, in citable form, before we publish the edited article. We will replace this *Accepted Manuscript* with the edited and formatted *Advance Article* as soon as it is available.

You can find more information about *Accepted Manuscripts* in the [Information for Authors](#).

Please note that technical editing may introduce minor changes to the text and/or graphics, which may alter content. The journal's standard [Terms & Conditions](#) and the [Ethical guidelines](#) still apply. In no event shall the Royal Society of Chemistry be held responsible for any errors or omissions in this *Accepted Manuscript* or any consequences arising from the use of any information it contains.

ARTICLE

Pb₆Ba₂(BO₃)₅X (X = Cl, Br): new borate halides with strong simulated optical anisotropies derived from Pb²⁺ and (BO₃)³⁻

Cite this: DOI: 10.1039/x0xx00000x

Received 00th January 2012,
Accepted 00th January 2012

DOI: 10.1039/x0xx00000x

www.rsc.org/

Lu Liu,^{a,b} Bingbing Zhang,^{a,b} Fangfang Zhang,^{*,a} Shilie Pan,^{*,a} Fangyuan Zhang,^{a,b}
Xingwen Zhang,^{a,b} Xiaoyu Dong,^{a,b} and Zhihua Yang^{*,a}

Two new borate halides, Pb₆Ba₂(BO₃)₅X (X = Cl, Br), have been synthesized by solid-state reactions and their structures determined by single-crystal X-ray diffraction. They are isostructural and feature 3D frameworks composed of the alternately stacking of the [PbBO] and [PbBOX] layers which are connected by 10-coordinated Ba atoms along the *c* direction. First principle calculations show that both compounds have large birefringence of 0.1582 and 0.1810 at 532 nm, respectively. The large birefringence originates from the strong optical anisotropies of the Pb²⁺ cations and (BO₃)³⁻ groups based on the real-space atom-cutting analysis. The IR and UV–Vis–NIR diffuse reflectance spectroscopies, as well as thermal stability analyses for both compounds are performed.

Introduction

Birefringent crystals as important materials in the optical communication industry have become hot research issues and attracted much attention in many fields such as optical polarizing components, optical isolators, circulators and beam displacers.¹ Up to now, a series of borate birefringent crystals have been found or commercially available. Commonly used borate birefringent material is α -BaB₂O₄ (BBO),² which has a broad transparent range from 189 to 3500 nm, a large birefringence (0.116 at 1064 nm) and high laser damage threshold. And there are also some potential borate birefringent crystals including Ca₃(BO₃)₂,³ YBa₃B₉O₁₈,⁴ Ba₂Mg(B₃O₆)₂,⁵ YAl₃(BO₃)₄,⁶ NaMgBO₃,⁷ etc. The Ca₃(BO₃)₂ crystal has a short UV transmittance cutoff at 180 nm, but its birefringence is small. YBa₃B₉O₁₈ has a wide range of 300 – 3000 nm, and a relative large birefringence about 0.11 in the visible range. Ba₂Mg(B₃O₆)₂ is recently reported as a new birefringent crystal with large birefringence (0.11 at 589 nm), and the UV absorption cut-off edge of is about 178 nm. Given this, it is still in urgent need of a new birefringent crystal with large birefringence and wide transmission range.

It is known that birefringence is related to the anisotropic polarizability of the structure,⁸ therefore, the structural groups with large polarizability anisotropy, for example, the coplanar and dense BO₃ groups can be selected for designing birefringent crystals.⁹ Taking the KBe₂BO₃F₂ (KBBF) crystal as an example, it demonstrates that the main contributions to the birefringence come from the (BO₃)³⁻ groups, whereas those from the K⁺ cations are negligible.¹⁰ At the same time, the Pb²⁺ cations can generate strong electronic anisotropy polarizability due to the stereochemically active lone pair effect.¹¹ Therefore, the incorporation of the Pb²⁺ cations and borate groups into one

compound is prone to produce crystals with large birefringence. However, there are few studies focusing on the effect of the Pb²⁺ cations on the birefringence.

In the current work, we explore the PbO–BaO–B₂O₃–NH₄X (X = Cl, Br) system and two new lead barium borate halides, Pb₆Ba₂(BO₃)₅X (X = Cl, Br), were successfully synthesized through the solid state reaction method. Isostructural Pb₆Ba₂(BO₃)₅Cl and Pb₆Ba₂(BO₃)₅Br reveal 3-dimension (3D) frameworks consisting of [PbBO] and [PbBOX] layers where the Ba²⁺ cations are resided in the interlayer. In this paper, the syntheses and characterizations of Pb₆Ba₂(BO₃)₅X are comprehensively investigated. The first principle calculations were performed on Pb₆Ba₂(BO₃)₅X and show that they have relatively large birefringence (0.1582 and 0.1810 at 532 nm, respectively). The origin of the large birefringence for the reported materials is discussed in detail by the real-space atom-cutting method.

Experimental

Solid-state Synthesis

Polycrystalline samples of Pb₆Ba₂(BO₃)₅X were synthesized by solid-state reactions method. Mixtures of NH₄Cl (8 mmol, 0.428 g), PbO (48 mmol, 10.714 g), BaCO₃ (16 mmol, 3.158 g) and H₃BO₃ (40 mmol, 2.473 g) for Pb₆Ba₂(BO₃)₅Cl, as well as NH₄Br (8 mmol, 0.784 g), PbO (48 mmol, 10.714 g), BaCO₃ (16 mmol, 3.158 g) and H₃BO₃ (40 mmol, 2.473 g) for Pb₆Ba₂(BO₃)₅Br, were packed into platinum crucibles and mixed thoroughly in an agate mortar, respectively. The powders were first preheated at 300 °C for 7 h. Then the mixture was gradually elevated to 530 °C, and dwelled at this temperature

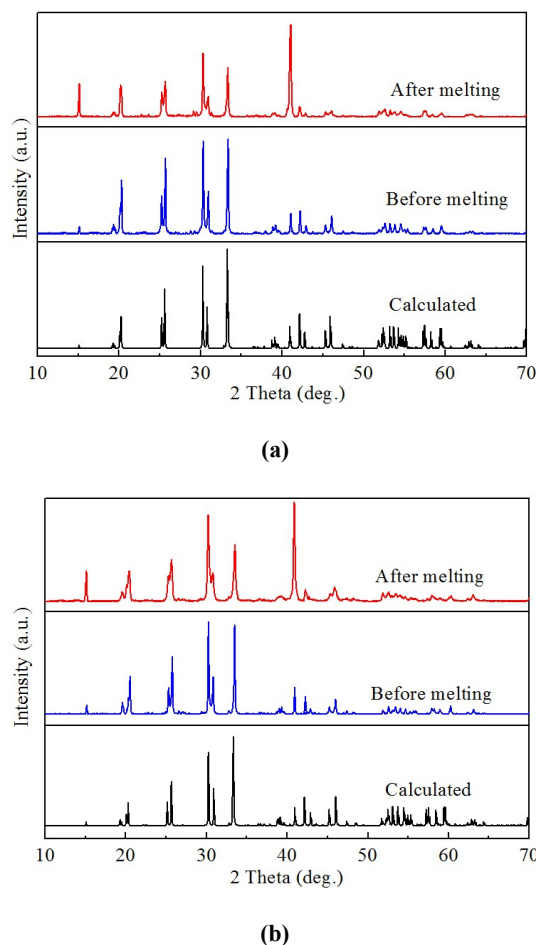


Figure 1. Powder XRD patterns of calculated, before melting and after melting for $\text{Pb}_6\text{Ba}_2(\text{BO}_3)_5\text{Cl}$ (a) and $\text{Pb}_6\text{Ba}_2(\text{BO}_3)_5\text{Br}$ (b).

for 72 h with several intermediate grindings and mixings. The purity of the samples was confirmed by powder X-ray diffraction (XRD) analyses. Powder XRD patterns for $\text{Pb}_6\text{Ba}_2(\text{BO}_3)_5\text{X}$ are shown in Figure 1, which are in good agreement with the calculated XRD patterns.

Single-crystal Growth

Single crystals of $\text{Pb}_6\text{Ba}_2(\text{BO}_3)_5\text{X}$ were grown by the spontaneous crystallization method. The crystals were grown from mixtures of NH_4Cl (2 mmol, 0.107 g), PbO (12 mmol, 2.679 g), BaCO_3 (4 mmol, 0.789 g) and H_3BO_3 (10 mmol, 0.618 g) for $\text{Pb}_6\text{Ba}_2(\text{BO}_3)_5\text{Cl}$, as well as NH_4Br (2 mmol, 0.196 g), PbO (12 mmol, 2.679 g), BaCO_3 (4 mmol, 0.789 g) and H_3BO_3 (10 mmol, 0.618 g) for $\text{Pb}_6\text{Ba}_2(\text{BO}_3)_5\text{Br}$. The starting materials were respectively loaded in the Pt crucibles which were put in a vertical programmable temperature furnace, and then the temperature was heated to 700 °C at a rate of 5 °C/min and kept for 10 h to guarantee that the solution mixed thoroughly and homogeneously. Later it was cooled down to the initial crystallization temperature 580 °C at a rate of 50 °C/h, and followed by cooling to 560 °C at the rate of 1 °C/h. Finally, the temperature was allowed to cool to room temperature at a rate of 10 °C/h. Hence a few of colorless

crystals of $\text{Pb}_6\text{Ba}_2(\text{BO}_3)_5\text{X}$ could be found from the solution, respectively.

Structure Determination

$\text{Pb}_6\text{Ba}_2(\text{BO}_3)_5\text{X}$ single-crystals with dimensions of $0.204 \times 0.088 \times 0.035 \text{ mm}^3$ and $0.201 \times 0.151 \times 0.098 \text{ mm}^3$ were respectively selected under microscope and the structure data were collected by single-crystal XRD on a Bruker SMART APEX II single-crystal diffractometer equipped with a 4K CCD-detector using Mo $K\alpha$ radiation at 296 (2) K and integrated with a SAINT-Plus program.¹² The numerical absorption corrections were carried out using the SADABS program for area detector.¹³ Then the crystal structures were solved by direct methods and refined in SHELX-97 crystallographic software package.¹⁴ All atoms were refined with anisotropic displacement parameters. The structures were checked for missing symmetry elements with PLATON.¹⁵ Crystal data and structure refinements are listed in Table 1. The atomic coordinates and equivalent isotropic displacement parameters are given in Table S1 in the Supporting Information. Selected bond lengths and angles for $\text{Pb}_6\text{Ba}_2(\text{BO}_3)_5\text{X}$ are listed in Table S2 in the Supporting Information.

Table 1. Crystal data and structure refinement for $\text{Pb}_6\text{Ba}_2(\text{BO}_3)_5\text{X}$ (X = Cl, Br).

Empirical formula	$\text{Pb}_6\text{Ba}_2(\text{BO}_3)_5\text{Cl}$	$\text{Pb}_6\text{Ba}_2(\text{BO}_3)_5\text{Br}$
Formula weight	1847.32	1891.78
Temperature / K	296(2)	296(2)
Crystal system	Monoclinic	Monoclinic
Space group	$C2/m$	$C2/m$
Unit cell dimensions	$a = 9.3155(7) \text{ \AA}$ $b = 5.3958(5) \text{ \AA}$ $c = 17.9757(17) \text{ \AA}$ $\beta = 101.172(6)^\circ$	$a = 9.306(5) \text{ \AA}$ $b = 5.388(3) \text{ \AA}$ $c = 17.994(9) \text{ \AA}$ $\beta = 101.513(6)^\circ$
$Z, V / \text{\AA}^3$	2, 886.42(13)	2, 884.2(8)
$D_{\text{cal.}} / \text{g} \cdot \text{cm}^{-3}$	6.92	7.11
Absorption coefficient / mm^{-1}	61.3	63.6
$F(000)$	1532	1568
Crystal size / mm^3	$0.204 \times 0.088 \times 0.035$	$0.201 \times 0.151 \times 0.098$
Limiting indices	$-10 \leq h \leq 10,$ $-6 \leq k \leq 5,$ $-21 \leq l \leq 18$	$-10 \leq h \leq 10,$ $-6 \leq k \leq 6,$ $-14 \leq l \leq 21$
Reflections unique (R_{int})	0.0617	0.0528
Completeness to theta / %	99.7	99.7
Goodness-of-fit on F^2	1.120	1.088
Final R indices [$F_o^2 > 2\sigma(F_o^2)$] ^a	$R_1 = 0.0465, wR_2 = 0.1033$	$R_1 = 0.0574, wR_2 = 0.1632$
R indices (all data) ^a	$R_1 = 0.0554, wR_2 = 0.1063$	$R_1 = 0.0633, wR_2 = 0.1717$
Largest diff. peak and hole / $e \cdot \text{\AA}^{-3}$	2.32 and -2.38	4.46 and -6.93

Powder X-ray Diffraction

Powder XRD analyses of $\text{Pb}_6\text{Ba}_2(\text{BO}_3)_5\text{X}$ were performed at room temperature in the angular range of $2\theta = 10 - 70^\circ$ with a scan step width of 0.02° and a fixed counting time of 1 s/step using an automated Bruker D2 PHASER X-ray

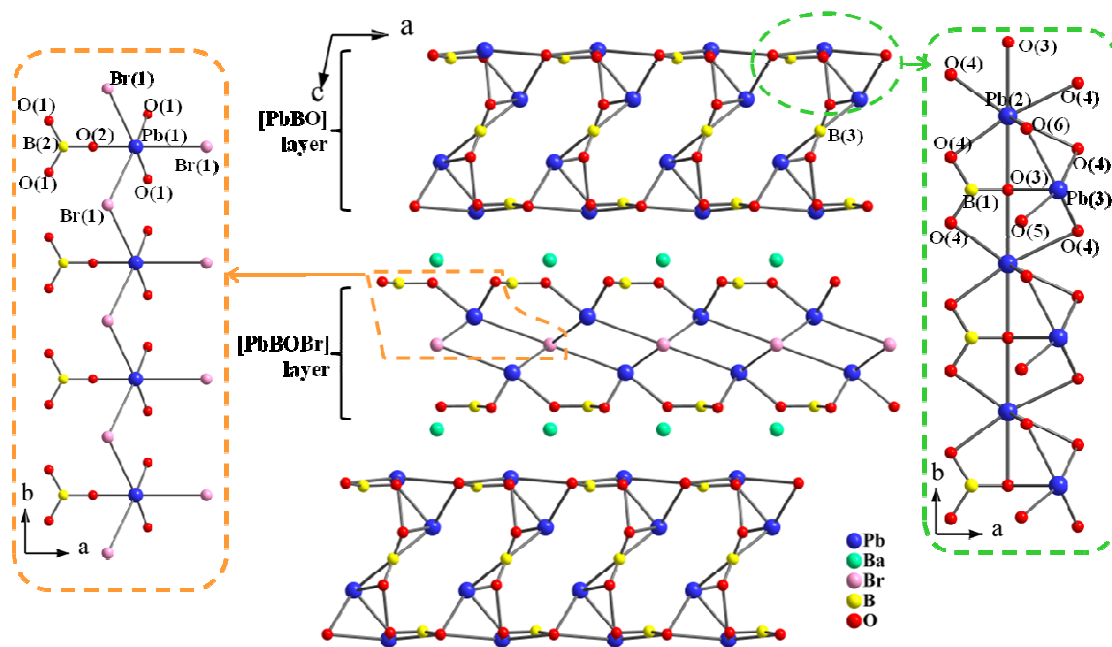


Figure 2. The crystal structure of $\text{Pb}_6\text{Ba}_2(\text{BO}_3)_5\text{Br}$.

diffractometer equipped with a diffracted beam monochromator set for Cu-K α radiation

Infrared Spectroscopy

The IR spectra were measured on a Shimadzu IR Affinity-1 Fourier transform IR spectrometer. The samples were respectively thoroughly mixed with dried KBr (6 mg of the sample and 590 mg of KBr) and pressed into discs, and the spectra were recorded in the range from 400 to 4000 cm^{-1} with a resolution of 2 cm^{-1} .

UV-Vis-NIR Diffuse Reflectance Spectroscopy

The diffuse reflectance data of the $\text{Pb}_6\text{Ba}_2(\text{BO}_3)_5\text{X}$ powder samples were respectively collected at room temperature on a Shimadzu SolidSpec-3700DUV UV-Vis-NIR Spectrophotometer with the spectral range from 190 to 2600 nm.

Thermal Analysis

The thermal analyses of $\text{Pb}_6\text{Ba}_2(\text{BO}_3)_5\text{X}$ were carried out on a NETZSCH STA 449C thermal analyzer instrument. The samples were respectively placed into Pt crucibles with a heating rate of 10 $^\circ\text{C}/\text{min}$ in an atmosphere of flowing N_2 from room temperature to 1000 $^\circ\text{C}$.

First-principles Calculations

The electronic structure of $\text{Pb}_6\text{Ba}_2(\text{BO}_3)_5\text{X}$ was investigated using the density functional theory (DFT) method based the *ab initio* implemented in the CASTEP package.¹⁶ The Perdew-Burke-Ernzerh of functional within the Generalized Gradient Approximation scheme was applied for the exchange-correlation potential.¹⁷ The Monkhorst-Pack grid¹⁸ was set at $3 \times 3 \times 1$ in the Brillouin zone (BZ) of the unit cell. For the purpose of achieving energy convergence, the plane-wave cutoff for a normal-conserving pseudopotential is 820.0 eV.¹⁹ And the valence electrons were provided by the package used.

Results and discussion

Crystal Structure

$\text{Pb}_6\text{Ba}_2(\text{BO}_3)_5\text{X}$ are isostructural and crystallize in the monoclinic system with space group $C2/m$. Therefore, only the structure of $\text{Pb}_6\text{Ba}_2(\text{BO}_3)_5\text{Br}$ is discussed in detail as are representative. Its crystal structure is illustrated in Figure 2. The asymmetric unit of the compound is composed of three crystallographically distinct lead sites, one crystallographically distinct barium site, one crystallographically distinct bromine site, three crystallographically distinct boron sites and six crystallographically distinct oxygen sites. The structure shows a complicated 3D network and it is characterized by the alternately stacking of the [PbBO] and [PbBOBr] layers which are connected by 10-coordinated Ba atoms along the *c* direction (Figure 2). In the [PbBO] layer, the $\text{Pb}(2)\text{O}_7$, $\text{Pb}(3)\text{O}_5$ polyhedra and $\text{B}(1)\text{O}_3$ groups connect with each other via

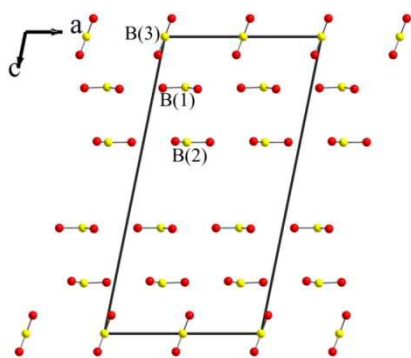


Figure 3. Arrangements of the BO_3 groups in $\text{Pb}_6\text{Ba}_2(\text{BO}_3)_5\text{X}$ viewed along the b direction.

sharing O(1), O(3) and O(4) to form a chain, which is further extended through the O(4) atoms along the a direction, and the connectivity is through bridging B(3), O(5) and O(6) atoms along the c direction. In the $[\text{PbBOBr}]$ layer, the $\text{Pb}(1)\text{O}_3\text{Br}_3$ polyhedra and $\text{B}(2)\text{O}_3$ groups link with each other to form a chain, and the chains further extending along a direction via O(1) atoms, whereas along the c direction the connectivity is via bridging Br atoms.

All kinds of planar BO_3 groups are parallel to the b -axis (Figure 3). At the same time, $\text{B}(1)\text{O}_3$ is parallel to $\text{B}(2)\text{O}_3$ whereas the plane of the $\text{B}(3)\text{O}_3$ and $\text{B}(2)\text{O}_3$ groups has dihedral angles of 71.2° . The ratio of the parallel $\text{B}(1)\text{O}_3$ and $\text{B}(2)\text{O}_3$ groups to the inclined $\text{B}(3)\text{O}_3$ groups is 4:1.

In the structure, the B atoms are all coordinated with three O atoms to form isolated BO_3 groups. It is worth noting that the O5, O5', O6 and O6' atoms in $\text{B}(3)\text{O}_3$ groups are generated by the 2-fold axis, and the sites of these atoms are half-occupied. As shown in Figure S1 in the Supporting Information, the $\text{B}(3)\text{O}_3$ group randomly adopts one of the orientations (up or down). The average lengths of the B-O bond in three types of the BO_3 groups are 1.363 Å, which is close to those observed in other known borates.^{20–22} It should be known that Pb(1) is not only bonded to three O atoms but also three Br atoms. Pb(2) and Pb(3) merely connect with seven or five O atoms to form distorted polyhedra, respectively. The Pb-O bonds range from 2.221–2.800 Å and the Pb-Br bond length 3.313 Å, which is normal in other compounds.²³ The Ba atom is bonded to nine O atoms and one Br atom, and the Ba-O bond lengths are in the range of 2.820–2.858 Å, the Ba-Br bond length is 3.488 Å.

Infrared Spectroscopy

IR spectra of $\text{Pb}_6\text{Ba}_2(\text{BO}_3)_5\text{X}$ between 400 and 4000 cm^{-1} were shown in Figure S2 in the Supporting Information. Referring to the literatures,²⁴ the peaks near 1384, 1163 for $\text{Pb}_6\text{Ba}_2(\text{BO}_3)_5\text{Cl}$ and 1369, 1159 cm^{-1} for $\text{Pb}_6\text{Ba}_2(\text{BO}_3)_5\text{Br}$ are attributed to the asymmetric and symmetric stretching vibrations for the BO_3 groups. The bands observed at 835 and 717 cm^{-1} for $\text{Pb}_6\text{Ba}_2(\text{BO}_3)_5\text{X}$ ($\text{X} = \text{Cl}, \text{Br}$) are related to the out-of-plane bending vibrations of B-O bonds in the BO_3 groups. These results are in agreement with other compounds containing BO_3 anionic groups.

UV–Vis–NIR Diffuse Reflectance Spectroscopy

The optical diffuse reflectance spectra of $\text{Pb}_6\text{Ba}_2(\text{BO}_3)_5\text{X}$ are shown in Figure S3. Absorption (K/S) data were calculated from the following Kubelka – Munk function:^{25, 26}

$$F(R) = (1 - R)^2 / 2R = K/S$$

Where R representing the reflectance, K is the absorption, and S the scattering. In a $F(R)$ versus E (eV) plot, extrapolating the band gaps of $\text{Pb}_6\text{Ba}_2(\text{BO}_3)_5\text{X}$ are 3.7, 3.6 eV, respectively.

Thermal Analysis

The TG-DSC curves of $\text{Pb}_6\text{Ba}_2(\text{BO}_3)_5\text{X}$ are shown in Figure S4. TG analysis studies indicate that $\text{Pb}_6\text{Ba}_2(\text{BO}_3)_5\text{Cl}$ and $\text{Pb}_6\text{Ba}_2(\text{BO}_3)_5\text{Br}$ do not show weight loss before 875 and 800 °C, respectively. Then they began to lose weight slowly, corresponding to the volatilization of halogenide formed by decomposition. In their DSC curves there are only one clear and strong endothermic peaks at 683 °C and 665 °C, which corresponds to the melting points of $\text{Pb}_6\text{Ba}_2(\text{BO}_3)_5\text{X}$ respectively. In addition, the polycrystalline powder of $\text{Pb}_6\text{Ba}_2(\text{BO}_3)_5\text{X}$ were packed into a Pt crucible and heated to 700 °C, and hold at this temperature for 6 h, respectively, then they were cooled to room temperature slowly. Analyses of the powder XRD pattern of the solidified melt show that the solid products are identical to that of the initial powder (Figure 1), which reveals the congruent melting behavior of both compounds.

Electronic Structure

The calculated energy bands of $\text{Pb}_6\text{Ba}_2(\text{BO}_3)_5\text{X}$ along the line of high symmetry points in the BZ are shown in Figure S5 in the Supporting Information. It is found that $\text{Pb}_6\text{Ba}_2(\text{BO}_3)_5\text{X}$ are indirect band gap compounds with the valence band (VB) maximum and the conduction band (CB) minimum located at different points. The calculated band gaps are 2.70 eV and 2.61 eV, while the experimental optical band gaps are 3.7 eV and 3.6 eV, respectively. It is well-known that the calculated band gap can cause quantitative underestimation of band due to the discontinuity of exchange-correlation energy.²⁷ In consequence, in the subsequent calculations of the linear optical properties, scissors of 1 eV and 0.84 eV are adopted for $\text{Pb}_6\text{Ba}_2(\text{BO}_3)_5\text{X}$.

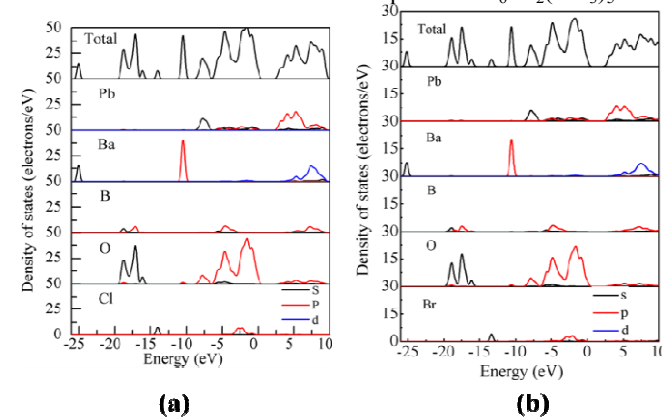


Figure 4. Total DOS and partial DOS of $\text{Pb}_6\text{Ba}_2(\text{BO}_3)_5\text{Cl}$ (a) and $\text{Pb}_6\text{Ba}_2(\text{BO}_3)_5\text{Br}$ (b).

The total and partial densities of states of $\text{Pb}_6\text{Ba}_2(\text{BO}_3)_5\text{X}$ are shown in Figure 4. It is obvious that the valence band ranging from -26.0 to -10.0 eV can be assigned to Ba 5s, 5p, B 2p, 2s, O 2s and Cl 3s / Br 4s states. The highest valence band and the lowest conduction band near the Fermi level (between -10.0 and 10.0 eV) should be valued, which determine most of the

optical character in a compound. We can see that in that region, the Pb 6s, 6p and B 2p states overlap with O 2p states completely, indicating the covalent interactions of Pb-O and B-O.

To further understand the correlation between microscopic electronic structure and macroscopic properties, the electronic localization function (ELF) of $\text{Pb}_6\text{Ba}_2(\text{BO}_3)_5\text{Br}$ is also been calculated. ELF plot for $\text{Pb}_6\text{Ba}_2(\text{BO}_3)_5\text{Br}$ as shown in Figure 5 clearly demonstrates “lobes” on the Pb^{2+} cations due to the electrostatic repulsion and Pb-O bonding character. The interactions that exist between the Pb and O atoms also indicated by DOS are present due to the highly asymmetric bonding feature for Pb atoms, which can be considered as the stereochemical effect of the lone pair of Pb^{2+} . And there is also nonisotropic charge localization in the B and O sites. It can be concluded that the O-influencing Pb^{2+} cations and $(\text{BO}_3)^{3-}$ anionic groups are the key to optical anisotropies in $\text{Pb}_6\text{Ba}_2(\text{BO}_3)_5\text{Br}$.

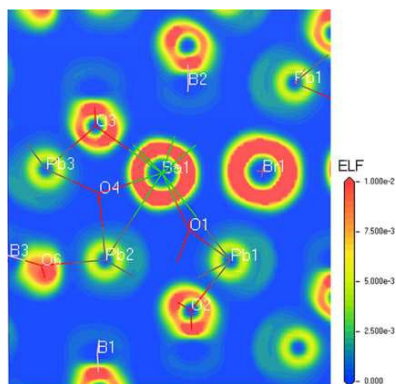


Figure 5. The ELF map of $\text{Pb}_6\text{Ba}_2(\text{BO}_3)_5\text{Br}$.

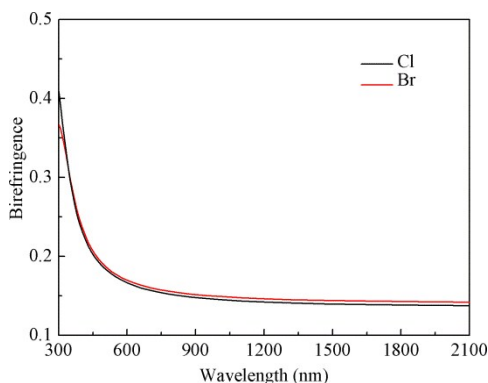


Figure 6. The birefringence of $\text{Pb}_6\text{Ba}_2(\text{BO}_3)_5\text{X}$ ($\text{X} = \text{Cl}, \text{Br}$).

Optical Properties

$\text{Pb}_6\text{Ba}_2(\text{BO}_3)_5\text{X}$ crystallizes in $2/m$ point group which belong to a negative biaxial crystal due to $n_y - n_x < n_x - n_z$. Firstly, we must confirm the principal dielectric axis if we want to calculate their linear optical properties. For example, in $\text{Pb}_6\text{Ba}_2(\text{BO}_3)_5\text{Br}$, the Y dielectric axis is superposed on the b crystallographic axis, but the principal dielectric axes X and Z are not related to any specific crystallographic directions. The included angle between the crystallographic axis a and the principal dielectric axis X in the ac plane was calculated to be 4.33° (Figure S6 in the Supporting Information). Through relevant rotation operation, the linear refractive indices of $\text{Pb}_6\text{Ba}_2(\text{BO}_3)_5\text{Br}$ were calculated in the principal dielectric axis

coordinate system. The obtained birefringence values against the wavelengths are plotted in Figure 6. It is clear that $\text{Pb}_6\text{Ba}_2(\text{BO}_3)_5\text{X}$ possess large birefringence with $\Delta n = 0.1582$ and $\Delta n = 0.1810$ at 532 nm, which demonstrates that they are potential birefringence materials.

Atom-cutting Analysis

To further elucidate and analyze the contribution of an ion (or an anionic group) to the birefringence, a real-space atom-cutting technique²⁸ was adopted, which has been widely used to analyze the linear refractive indices and SHG coefficients of many borate crystals, such as BBO, $\text{Li}_4\text{Sr}(\text{BO}_3)_2$,²⁹ $\text{BaAlBO}_3\text{F}_2$,³⁰ $\text{Bi}_2\text{ZnOB}_2\text{O}_6$ ³¹ and so on.³² The cutting radii of Pb, Ba, B, O, Cl and Br atoms are set as 1.2, 1.35, 0.82, 1.4, 1.81 and 1.95 Å, respectively. The calculated refractive indices and birefringence of $\text{Pb}_6\text{Ba}_2(\text{BO}_3)_5\text{Cl}$ using the “atom-cutting” method are listed in Table S3 in the supporting information. As shown in it, the contribution to the birefringence from all $(\text{BO}_3)^{3-}$ groups is about 56.5%. The contribution of the Pb^{2+} cations is about 27.1% while the contributions of Ba^{2+} and Cl^- are small. The calculated refractive indices and birefringence of $\text{Pb}_6\text{Ba}_2(\text{BO}_3)_5\text{Br}$ using the “atom-cutting” method are listed in Table 2. As shown in it, the contribution to the birefringence from all $(\text{BO}_3)^{3-}$ groups is about 48.6%. The contribution of the Pb^{2+} cations is about 48.2% while the contributions of Ba^{2+} , Br^- are negligibly small. From the above analysis, it is found that the contributions to optical anisotropies follow the trend of $(\text{BO}_3)^{3-} \approx \text{Pb}^{2+} \gg \text{Ba}^{2+}, \text{X}^-$.

Table 2. Atom-cutting analysis and calculated birefringence at 532 nm for $\text{Pb}_6\text{Ba}_2(\text{BO}_3)_5\text{Br}$.

Species	n_x	n_y	n_z	Δn
B(1)O ₃ , B(2)O ₃	1.6442	1.6946	1.5089	0.1857
B(3)O ₃	1.2385	1.2871	1.2357	0.0514
All $(\text{BO}_3)^{3-}$	1.7067	1.7476	1.6301	0.1175
Pb^{2+}	1.5326	1.5565	1.4401	0.1164
$\text{Ba}^{2+}, \text{Br}^-$	1.2189	1.2127	1.2111	0.0078
sum				0.2417
Calcd.	2.3127	2.3175	2.1365	0.1810

Structure-property Relationship

To better understand the contribution of the $(\text{BO}_3)^{3-}$ groups, paralleled and slant BO_3 groups were cut as the research units for $\text{Pb}_6\text{Ba}_2(\text{BO}_3)_5\text{Br}$, respectively. The calculations demonstrate that the birefringence of paralleled B(1)O₃ and B(2)O₃ groups is 0.1857, which is much bigger than 0.0514 of slant B(3)O₃ groups. As a result, the large optical anisotropy of the BO_3 groups mainly comes from the paralleled B(1)O₃ and B(2)O₃ groups. In addition, the high density can further explain why the contribution from the BO_3 groups is large. The density of structural units BO_3 is 0.0113 per unit volume which is higher than that in KBBF (0.00946 per unit volume, 0.070 at 532 nm). Generally, the B-O groups have a great significance for the birefringence of borates. It is rare that the birefringence coming from the contribution of the Pb^{2+} cations is also very large. For

example, in PbBiBO_4 ,³³ the BO_3 groups contribute 77% and Bi_2O_2 groups contribute 18% to its birefringence, which means that there is almost no contribution from the Pb^{2+} cations. In $\text{Pb}_2\text{BO}_3\text{F}$,³³ the contribution of BO_3 groups to birefringence is about 80%, while the Pb and F ions contribute only 20%. But, interestingly, in $\text{Pb}_6\text{Ba}_2(\text{BO}_3)_5\text{Br}$, the contribution to its birefringence derived from the Pb^{2+} cations (48.2%) is nearly equal to that of the $(\text{BO}_3)^{3-}$ groups (48.6%), respectively (Table 2). The optical anisotropies from the Pb^{2+} cations are strongly dependent on the stereochemically active lone-pair and the high content of Pb^{2+} .

Otherwise, from Table 2, we can see that for the Pb^{2+} cations and the $(\text{BO}_3)^{3-}$ groups, the smallest values of refractive indices arise from the direction of the z axis and the maximum appears on the y axis. It can be concluded that the Pb^{2+} cations and the $(\text{BO}_3)^{3-}$ groups make a mutual enhancement of optical anisotropies.

Conclusion

In summary, two new borate halides, $\text{Pb}_6\text{Ba}_2(\text{BO}_3)_5\text{X}$ have been synthesized successfully and their single crystals have been grown by the high temperature spontaneous crystallization method for the first time. They are isostructural and feature 3D frameworks that consist of [PbBO] and [PbBOX] layers which are connected by 10-coordinated Ba atoms along the c direction. The calculated results suggest that both compounds have large birefringence of 0.1582 and 0.1810 at 532 nm, respectively. To further confirm respective contributions to the total optical properties, we did the calculation by the real-space atom cutting method. The results demonstrate that the Pb^{2+} cations and the $(\text{BO}_3)^{3-}$ groups are responsible for overall birefringence in $\text{Pb}_6\text{Ba}_2(\text{BO}_3)_5\text{Br}$. The growth of large crystals for further physical property studies is ongoing.

Acknowledgements

This work is supported by the Xinjiang International Science & Technology Cooperation Program (20146001), the NSFC (Grant Nos. 51425206), National Natural Science Foundation of China (Grant Nos. 21301189, U1129301, 51172277, 11104344), the West Light Foundation of CAS (GrantNo.ZDXM-2014-01), the Xinjiang Program of Cultivation of Young Innovative Technical Talents (2013731018), the Foundation of the Youth Innovation Promotion Association of CAS, 973 Program of China (Grant No. 2014CB648400), and the Funds for Creative Cross & Cooperation Teams of CAS.

Notes and references

^aKey Laboratory of Functional Materials and Devices for Special Environments of CAS, Xinjiang Key Laboratory of Electronic Information Materials and Devices, Xinjiang Technical Institute of Physics & Chemistry of CAS, 40-1 South Beijing Road, Urumqi 830011, China. E-mail: ffzhang@ms.xjb.ac.cn (Fangfang Zhang); slpan@ms.xjb.ac.cn (Shilie Pan). Tel: (+86)991-3674558, Fax: (+86)991-3838957

^b Address here. University of Chinese Academy of Sciences, Beijing 100049, China.

† Electronic Supplementary Information (ESI) available: [CCDC-number 1030292 for $\text{Pb}_6\text{Ba}_2(\text{BO}_3)_5\text{Cl}$; CCDC-number 1030293 for $\text{Pb}_6\text{Ba}_2(\text{BO}_3)_5\text{Br}$]; crystal data (CIF files); atomic coordinates ($\times 10^4$) and equivalent isotropic displacement parameters ($\text{\AA}^2 \times 10^3$) for $\text{Pb}_6\text{Ba}_2(\text{BO}_3)_5\text{X}$; selected bond lengths (\AA) and angles (deg.) for $\text{Pb}_6\text{Ba}_2(\text{BO}_3)_5\text{X}$; Atom-cutting analysis and calculated birefringence at 532 nm for $\text{Pb}_6\text{Ba}_2(\text{BO}_3)_5\text{Cl}$. scheme showing the substructures of $\text{B}(3)\text{O}_3$ groups; IR spectra of $\text{Pb}_6\text{Ba}_2(\text{BO}_3)_5\text{X}$; UV-Vis-NIR diffuse reflectance spectra of $\text{Pb}_6\text{Ba}_2(\text{BO}_3)_5\text{X}$; TG-DSC curves of $\text{Pb}_6\text{Ba}_2(\text{BO}_3)_5\text{X}$; band structure of $\text{Pb}_6\text{Ba}_2(\text{BO}_3)_5\text{X}$; relative orientation of the indicatrix axes to the crystallographic axes in $\text{Pb}_6\text{Ba}_2(\text{BO}_3)_5\text{Br}$. See DOI: 10.1039/b000000x/

- (a) E. Hecht, *Optics*, Addison-Wesley, 1998. (b) G. Chartier, Introduction to Optics, Springer Science + Business Media Inc, 1995.
- (a) V. P. Solntsev, E. G. Tsvetkov, V. A. Gets and V. D. Antsygin, *J. Cryst. Growth*, 2002, **236**, 290–296. (b) G. Q. Zhou, J. Xu, X. D. Chen, H. Y. Zhong, S. T. Wang, K. Xu, P. Z. Deng and F. X. Gan, *J. Cryst. Growth*, 1998, **191**, 517–519. (c) S. F. Wu, G. F. Wang, J. L. Xie, X. Q. Wu, Y. F. Zhang and X. Lin, *J. Cryst. Growth*, 2002, **245**, 84–86. (d) R. Appel, C. D. Dyer and J. N. Lockwood, *Appl. Opt.*, 2002, **41**, 2470–2480.
- S. Y. Zhang, X. Wu, Y. T. Song, D. Q. Ni, B. Q. Hu and T. Zhou, *J. Cryst. Growth*, 2003, **252**, 246–250.
- Z. H. Zhang, J. J. Yang, M. He, X. F. Wang and Q. Li, *Appl. Phys. Lett.*, 2009, **92**, 171903.1–171903.3.
- R. K. Li and Y. Y. Ma, *CrystEngComm.*, 2012, **14**, 5421–5424.
- Y. H. Wang, L. L. Wang and H. D. Li, *J. Appl. Phys.*, 2007, **102**, 013711.1–013711.5.
- L. Wu, Y. Zhang, Y. F. Kong, T. Q. Sun, J. J. Xu and X. L. Chen, *Inorg. Chem.*, 2007, **46**, 5207–5211.
- F. Qin and R. K. Li, *J. Cryst. Growth*, 2011, **318**, 642–644.
- (a) Z. S. Lin, Z. Z. Wang, C. T. Chen and M. H. Lee, *J. Appl. Phys.*, 2001, **90**, 5585–5590. (b) L. Kang, S. Y. Luo, H. W. Huang, T. Zheng and C. T. Chen, *J. Phys.: Condens. Matter*, 2012, **24**, 335503. (c) Z. Wang, M. Zhang, S. L. Pan, Z. H. Yang, H. Zhang, B. B. Zhang, Y. Wang, J. Kang and X. X. Lin, *New J. Chem.*, 2014, **38**, 3035–3041. (d) R. K. Li, *Z. Kristallogr.*, 2013, **228**, 526–531.
- Z. S. Lin, Z. Z. Wang, C. T. Chen, S. K. Chen and M. H. Lee, *Chem. Phys. Lett.*, 2003, **367**, 523–527.
- F. L. Tan and R. K. Li, *J. Synth. Cryst.*, 2009, **38**, 26–32.
- SAINTE*, version 7.60A; Bruker Analytical X-ray Instruments, Inc.: Madison, WI, 2008.
- R. H. Blessing, *Acta Crystallogr. Sect. A*, 1995, **51**, 33–38.
- G. M. Sheldrick, *SHELXTL*, version 6.14; Bruker Analytical X-ray Instruments, Inc.: Madison, WI, 2003.
- A. L. Spek, *J. Appl. Crystallogr.*, 2003, **36**, 7–13.
- S. J. Clark, M. D. Segall, C. J. Pickard, P. J. Hasnip, M. J. Probert, K. Refson and M. C. Payne, *Z. Kristallogr.*, 2005, **220**, 567–570.
- J. P. Perdew, K. Burke and M. Ernzerhof, *Phys. Rev. Lett.*, 1996, **77**, 3865–3868.
- H. J. Monkhorst and J. D. Pack, *Phys. Rev. B*, 1976, **13**, 5188–5192.
- D. Vanderbilt, *Phys. Rev. B*, 1990, **41**, 7892–7895.
- (a) S. L. Pan, J. P. Smit, M. R. Marvel, C. L. Stern, B. Watkins, K. R. Poeppelmeier, *Mater. Res. Bull.*, 2006, **41**, 916–924. (b) X. W. Zhang, H. W. Yu, H. P. Wu, S. L. Pan, A. Q. Jiao, B. B. Zhang and Z. H.

- Yang, *RSC Adv.*, 2014, **4**,13195–13200. (c) Z. Wang, M. Zhang, S. L. Pan, Y. Wang, H. Zhang, and Z. H. Chen, *Dalton Trans.*, 2014, **43**,2828–2834. (d) S. J. Han, Y. Wang, S. L. Pan, X. Y. Dong, H. P. Wu, J. Han, Y. Yang, H. W. Yu and C. Y. Bai, *Cryst. Growth Des.*, 2014, **14**, 1794–1810.
- 21 (a) L. L. Liu, X. Su, Y. Yang, S. L. Pan, X. Y. Dong, S. J. Han, M. Zhang, J. Kang and Zhihua Yang, *Dalton Trans.*, 2014, **43**, 8905–8910. (b) F. Kong, S. P. Huang, Z. M. Sun, J. G. Mao and W. D. Cheng, *J. Am. Chem. Soc.*, 2006, **128**, 7750–7751. (d) S. C. Wang and N. Ye, *J. Am. Chem. Soc.*, 2011, **133**, 11458–11461. (e) L. Cheng, Q. Wei, H. Q. Wu, L. J. Zhou and G. Y. Yang, *Chem. Eur.J.*, 2013, **19**, 17662–17667. (f) H. X. Zhang, J. Zhang, S. T. Zheng, G. Y. Yang, *Cryst. Growth Des.*, 2005, **5**, 157–161.
- 22 (a) H. P. Wu, H. W. Yu, Z. H. Yang, X. L. Hou, X. Su, S. L. Pan, K. R. Poeppelmeier and J. M. Rondinelli, *J. Am. Chem. Soc.*, 2013, **135**, 4215. (b) H. P. Wu, S. L. Pan, K. R. Poeppelmeier, H. Y. Li, D. Z. Jia, Z. H. Chen, X. Y. Fan, Y. Yang, J. M. Rondinelli and H. S. Luo, *J. Am. Chem. Soc.*, 2011, **133**, 7786. (c) L. Y. Li, G. B. Li, Y. X. Wang, F. H. Liao and J. H. Lin, *Inorg. Chem.*, 2005, **44**, 8243. (d) R. H. Cong, J. L. Sun, T. Yang, M. R. Li, F. H. Liao, Y. X. Wang and J. H. Lin, *Inorg. Chem.*, 2011, **50**, 5098. (e) J. H. Zhang, F. Kong and J. G. Mao, *Inorg. Chem.*, 2011, **50**, 3037–3043.
- 23 (a) L. Y. Dong, S. L. Pan, Y. Wang, H. W. Yu, S. J. Han and M. Zhang, *Inorg. Chem.*, 2013, **52**, 11377–11384. (b) L. Y. Dong, S. L. Pan, H. P. Wu, X. Su, H. W. Yu, Y. Wang, Z. H. Chen, Z. J. Huang and Z. H. Yang, *J. Solid State Chem.*, 2013, **204**, 64–69.
- 24 (a) X. Y. Dong, L. Cui, Y. J. Shi, S. L. Pan, Z. X. Zhou, Z. H. Yang, B. B. Zhang, X. Z. Jiang, Y. Yang, Z. H. Chen and Z. J. Huang, *Z. Anorg. Allg. Chem.*, 2013, **639**, 988–993. (b) H. W. Yu, H. P. Wu, S. L. Pan, Y. Wang, Z. H. Yang and X. Su, *Inorg. Chem.*, 2013, **52**, 5359–5365.
- 25 P. Kubelka and F. Z. Munk, *Tech. Phys.*, 1931, **12**, 593–601.
- 26 J. Tauc, *Mater. Res. Bull.*, 1970, **5**, 721–729.
- 27 M. K. Y. Chan and G. Ceder, *Phys. Rev. Lett.*, 2010, **105**, 196403–19406.
- 28 J. Lin, M. H. Lee, Z. P. Liu, C. T. Chen and C. J. Pickard, *Phys. Rev. B*, 1999, **60**, 13380–13389.
- 29 S. G. Zhao, P. F. Gong, L. Bai, X. Xu, S. Q. Zhang, Z. H. Sun, Z. S. Lin, M. C. Hong, C. T. Chen and J. H. Luo, *Nat. Commun.*, 2014, **5**,4019.
- 30 A. H. Reshak, D. Stys, S. Auluck and I. V. Kityk, *Phys. Chem. Chem. Phys.*, 2011, **13**, 2945–2952.
- 31 X. Su, Y. Wang, Z. H. Yang, X. C. Huang, S. L. Pan, F. Li and M. H. Lee, *J. Phys. Chem. C*, 2013, **117**, 14149–14157.
- 32 B. B. Zhang, Z. H. Yang, Y. Yang, M. H. Lee, S. L. Pan, Q. Jing and X. Su, *J. Mater. Chem. C*, 2014, **2**, 4133–4141.
- 33 Q. Bian, Z. H. Yang, L. Y. Dong, S. L. Pan, H. Zhang, H. P. Wu, H. W. Yu, W. W. Zhao and Jing, Q. *J. Phys. Chem. C*, 2014, **118**, 25651–25657.

Abstract Graphics

Manuscript title: $\text{Pb}_6\text{Ba}_2(\text{BO}_3)_5\text{X}$ ($\text{X} = \text{Cl}, \text{Br}$): new borate halides with strong simulated optical anisotropies derived from Pb^{2+} and $(\text{BO}_3)^{3-}$

Author: Lu Liu,^{a,b} Bingbing Zhang,^{a,b} Fangfang Zhang,^{*a} Shilie Pan,^{*a} Fangyuan Zhang,^{a,b} Xingwen Zhang,^{a,b} Xiaoyu Dong,^{a,b} and Zhihua Yang^{*a}

Two new lead barium borate halides, $\text{Pb}_6\text{Ba}_2(\text{BO}_3)_5\text{X}$ ($\text{X} = \text{Cl}, \text{Br}$), were successfully synthesized by solid-state reactions. First principle calculations on them show that they have large birefringence of 0.1582 and 0.1810 at 532 nm. The birefringence originates from the strong optical anisotropies of the Pb^{2+} cations and $(\text{BO}_3)^{3-}$ groups based on the real-space atom-cutting analysis.

